

Construction of Experimental Method for Airflow Analysis inside a Soundproofing Ventilation Unit

Yuichi Tanaka^{1*}, Norihiro Hayashida¹, Keisuke Masuda¹, Sohei Nishimura¹, Teiichi Tanaka¹

¹National Institute of Technology, Kumamoto College, Hirayamashin-Machi, Yatsushiro, Kumamoto, 2627, Japan

*Corresponding Author: Yuichi Tanaka, National Institute of Technology, Kumamoto College, Japan, y-tanaka@kumamoto-nct.ac.jp

ABSTRACT

A soundproof window with ventilation is proposed to solve the road noise problem in subdeveloped countries of tropical regions. However, to gain a practical attenuation amount, it is necessary to use noise-absorbing material and introduce partition boards and perforated boards; these influence the ventilation inside the unit. Therefore, the airflow inside the soundproofing unit should be verified to minimise this influence. This study aims at understanding the airflow inside a soundproofing ventilation unit (SVU) with a particle image velocimetry PIV system. By measuring the airflow at three different spots of an SVU with PIV, we verified the airflow distribution inside the SVU at each inflow velocity. In addition, by comparing the measurement result at the outflow port with PIV and a hot wire anemometer, we verified the measurement accuracy. Finally, we changed the laser pulse interval and analysis area to verify how they affect the measurement values.

Keywords: Soundproofing Ventilation Unit, Airflow, PIV, Hot wire anemometer

INTRODUCTION

Significant economic development in recent years has aggravated environmental problems such as road noise in subdeveloped countries of tropical regions [1-2]. Because air conditioning has not yet been fully disseminated in most of these countries, double-ventilated windows, made of two doors, have been widely adopted. These types of windows, however, are not capable of dealing with the current road noise problem. To solve this problem, Nasu and Nishimura proposed a soundproof window with ventilation [3]. In their study, they conducted a three-dimensional analysis of sound propagation inside a soundproofing unit and demonstrated noise reduction both theoretically and experimentally.

However, to gain a practical attenuation amount, it is necessary to use noise-absorbing material and introduce partition boards and perforated boards; these influence the ventilation inside the unit. Therefore, the airflow inside the soundproofing unit should be verified to minimise this influence. If we succeed in understanding the airflow inside the soundproofing unit, we believe we can develop a soundproofing

unit with both soundproof and ventilation capacity by installing noise-absorbing material in positions that do not interfere with the ventilation.

Therefore, this study aims at understanding the airflow inside a soundproofing ventilation unit (SVU) with a particle image velocimetry PIV system.

PARTICLE IMAGE VELOCIMETRY

PIV is a method that measures the velocity vector of a measurement space two dimensionally or three dimensionally without contact. Figure 1 shows the principle of PIV measurement.

First, tracer particles that track fluids are mixed into the flow of a liquid or gas. Then, a laser beam is irradiated to visualise the flow, and a high-speed camera captures images of the particles. From the continuous images, the displacement vector dx during an infinitesimal time dt is obtained, and the velocity vector dx/dt is estimated. The two PIV methods include the image correlation method and the particle tracking method. The first tracks multiple particles within the analysis area and the latter tracks a single particle [4].

Construction of Experimental Method for Airflow Analysis inside a Soundproofing Ventilation Unit

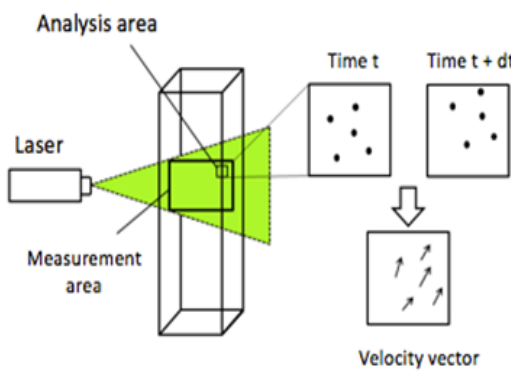


Figure 1. Principle of PIV measurement

OUTLINE OF PIV MEASUREMENT

Outline of a Soundproofing Ventilation Unit

We built an SVU with 2-mm-thick transparent acrylic resin boards for the measurement. Figure 2 shows the model and its dimensions. The internal dimensions of the model are W 140 mm \times D 70 mm \times H 560 mm, and we made an inflow port of 120 mm \times 35 mm at the bottom and an outflow port of 120 mm \times 82 mm at the front.

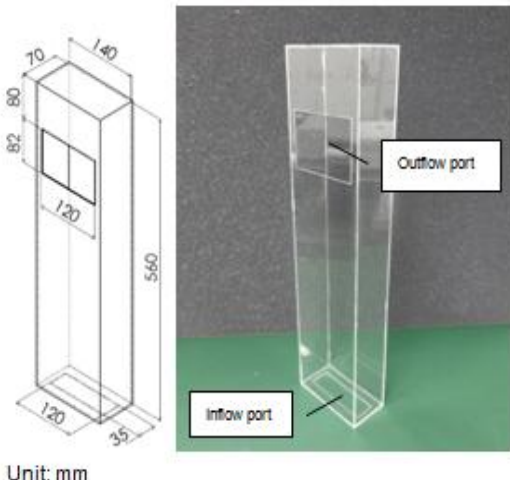


Figure 2. Model outline

Measurement Method

Figure 3 shows an outline of the PIV system used for the measurement. In the measurement, air is blown into the model at a constant speed by controlling the voltage of a DC fan installed under the SVU. At the same time, an oil mist of 1 μm in diameter, generated by an aerosol generator (a particle generator) manufactured by LaVision, is supplied as tracer particles. A laser beam irradiates the particles, whose behaviour is photographed by a high-speed camera. Finally, the PIV analysis is carried out [5-6]. Table 1 shows the conditions of PIV measurement. We used a software package called DaVis 8.0 for

the PIV analysis to calculate the velocity vector image on a two-dimensional section using the correlation method. The names of the equipment used in the experiment are indicated in Table 2.

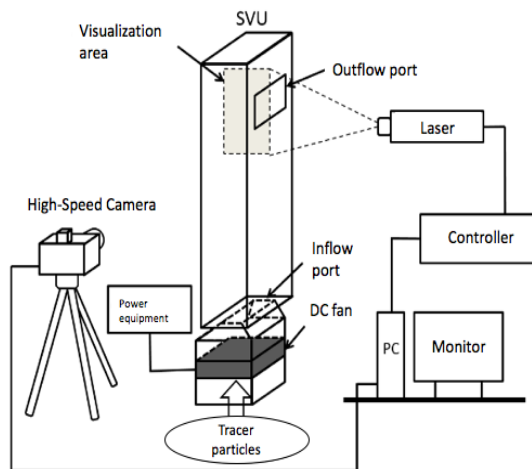


Figure 3. Outline of PIV system

Table 1. Conditions of PIV measurement and analysis

Measurement method	Double frames
Measurement interval	$f = 5 \text{ Hz}$
Measurement length	2 s
Laser pulse interval	200 μs
Analysis area	32 \times 32 pixels
Overlap	75%

Table 2. Experimental equipment

PIV system	FlowMaster2D-PIV (LaVision GmbH)
Camera	Imager sCMOS
Laser	Double Pulse Nd: YAG Laser
Software	DaVis 8.0 Software
Particle generator	Aerosol Generator
Voltage device	Regulated dc power supply PR18-3A (Kenwood)
DC fan	DC Fan Motor ASFN80372 (Panasonic)
Hot wire anemometer	Anemometer LTE Model 6006 (Kanomax Japan)

EXPERIMENT METHOD

Determining the Airflow Distribution with PIV Measurement

In this experiment, we carried out the PIV measurement by changing the voltage of the DC fan to three levels—6 V, 12 V, and 24 V—under the conditions indicated in Table 1. We observed that the airflow inside the SVU changes according to the variation in inflow velocity. We defined the measurement area as three two-dimensional sections indicated in Figure 4.

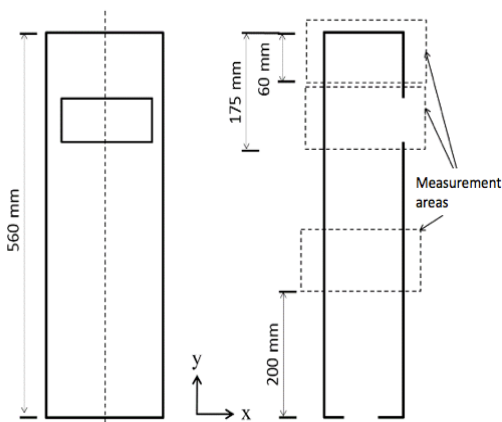


Figure4. Measurement areas

Table3. Inflow velocity at each voltage

Inflow velocity	6 V, $U_{in1} = 0.326 \text{ m/s}$
	12 V, $U_{in2} = 0.912 \text{ m/s}$
	24 V, $U_{in3} = 2.025 \text{ m/s}$

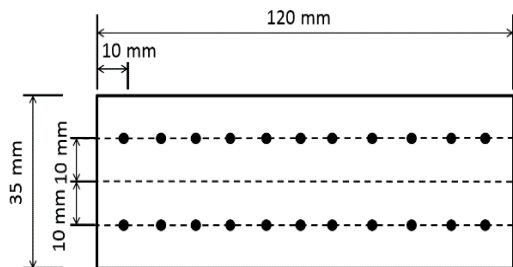


Figure5. Measurement points at inflow port

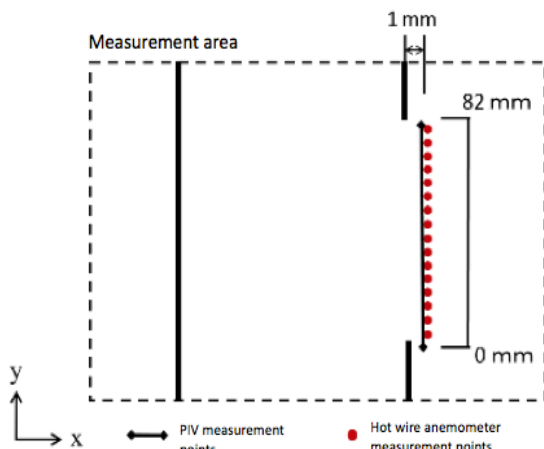


Figure6. Measurement points at outflow port

Table 3 shows the inflow velocity with each DC fan voltage. These numbers are the average of 22 measurements of the wind speed at the inflow port, obtained by a hot wire anemometer at 10 mm intervals in the horizontal direction, as indicated in Figure 5.

Comparison of Measurement Values obtained by PIV and Hot Wire Anemometer

In the PIV measurement, we set the photography area around the outflow port, where it is easy to compare with the hot wire

anemometer, and the measurement position in the section between 0 and 82 mm of the outflow port, as indicated in Figure 6. The measurement conditions are indicated in Table 1.

Using the hot wire anemometer, we measured 16 points in the central section of the outflow port, between 0 and 82 mm at 5-mm intervals starting at 1 mm, as indicated in Figure 6. The measurement value is the average of 30 measurements taken at each point.

Change in Measurement Values according to Measurement Conditions

To verify the change in measurement values according to the measurement conditions, we acquired additional pictures for a PIV measurement similar to that described above. Under the conditions shown in Table 1, we observed the changes in measurement values when only the laser pulse interval was changed from 200 μs to 500 μs and 800 μs , and when only the analysis area was reduced from 32 \times 32 to 16 \times 16 pixels.

MEASUREMENT RESULTS AND DISCUSSION

Airflow Change Inside SVU at Different Velocities

In this experiment, we set the photographing time with PIV to 2 s, and the photographing interval to 5 Hz. Therefore, with one shooting, it is possible to obtain 10 images as the instantaneous wind speed vector distribution. The average wind speed vector distribution is obtained by averaging this instantaneous wind speed vector distribution. We verified the airflow change by observing both the instantaneous wind speed vector distribution and the average wind speed vector distribution.

Airflow Change near the Outflow Port

Figure 7 shows an instantaneous wind speed vector distribution schematic near the outflow port at a voltage of 24 V in order of photographing time with PIV. As Figure 7 (a) shows, in the lower part near the exit, the flow in the Y direction is strong, but in the upper part of the exit, the vectors lean toward the X direction, flowing in a direction vertical to the exit. In Figure 7 (b), the flow in the X direction decreases, and the air flows diagonally to the right owing to a strong influence of the flow in the Y direction from the lower part. In Figure 7 (c), it returns to a flow similar to that of (a). Therefore, because images (a) to (c) show a similar pattern, it is possible to conclude that the phenomenon above is repeated periodically.

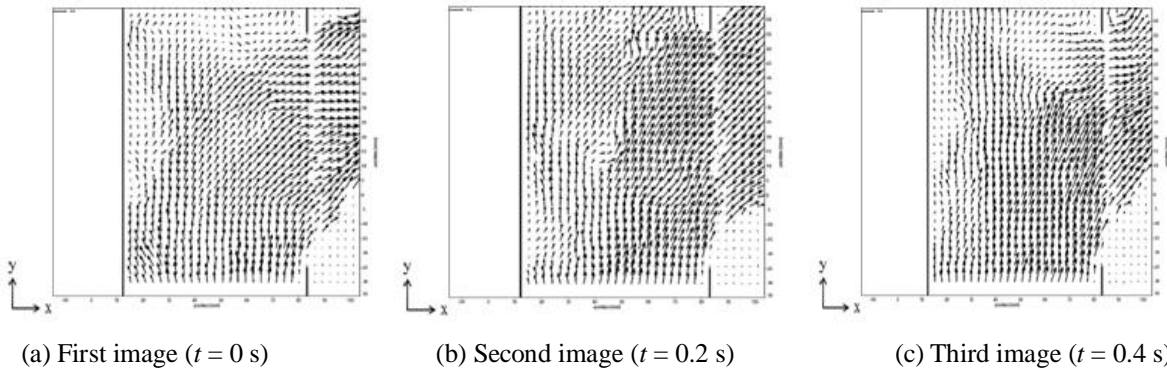


Figure 7. Instantaneous wind speed vector distribution near outlet port (DC Voltage: 24 V)

We will omit the schematic, but a similar pattern was repeated in the instantaneous wind speed vector distribution of 6 V and 12 V. In addition, with shootings of 2 s—despite minor variations between the shootings—we were able to

confirm the pattern of airflow change four times at 24 V, three times at 12 V, and twice at 6 V. From these findings, it is possible to conclude that the lower the inflow velocity, the longer the airflow change period.

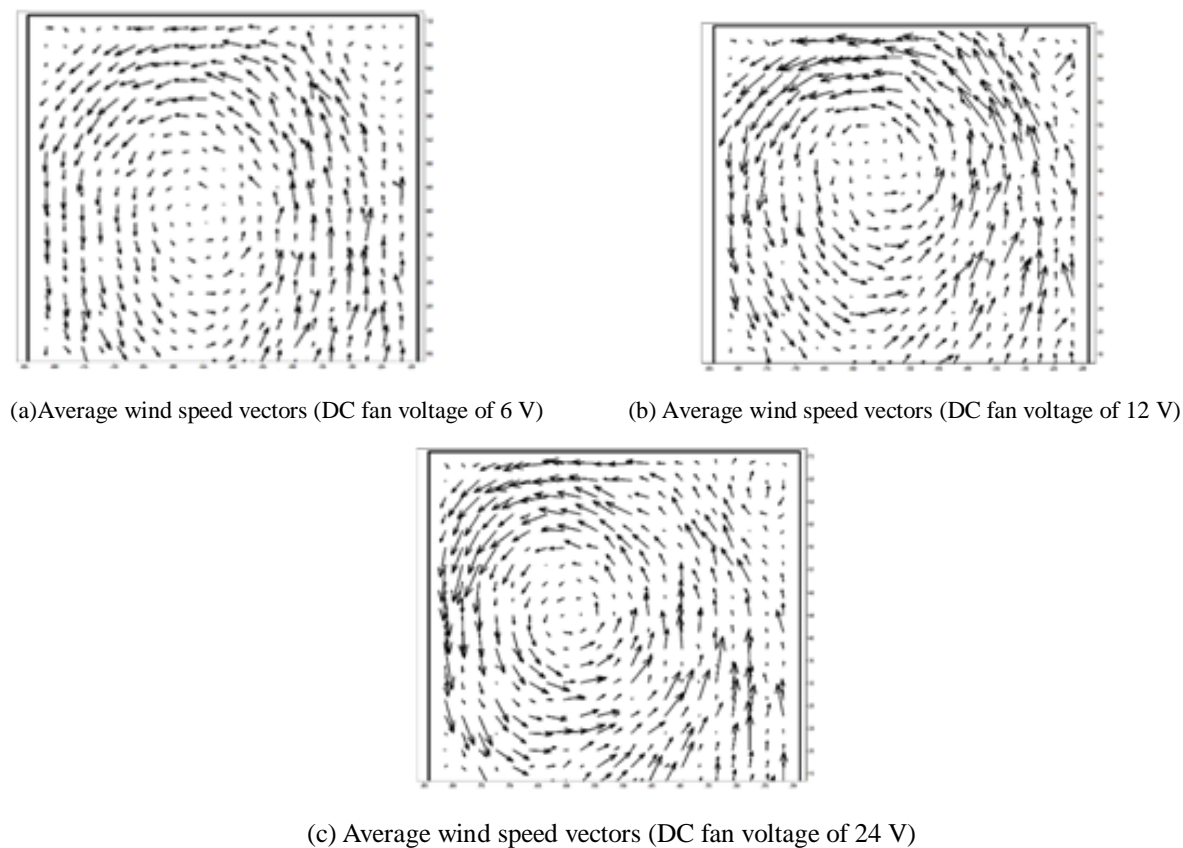


Figure 8. Average wind speed vector at top of SVU

Airflow Change at the Top of an SVU

Figure 8 shows the average wind speed vector distribution at the top of an SVU at each voltage. As Figure 8 shows, at the top of the SVU, the flow from the lower part runs along the wall at all voltages, and when the outflow direction is set to the right, a counter clockwise swirl is formed.

One of the differences when different velocities are applied is the position at which the swirl occurs. When the DC motor voltage is 6 V, the

swirl is formed near the centre. However, as the velocity increases, it is possible to verify that the swirl gradually moves toward the wall opposite to the outflow port. This is probably because the higher velocity increased the flow to the upper part of the SVU. In addition, although we omit the schematic, the instantaneous wind speed vectors indicate that the velocity change of this swirl is almost identical to the period of the flow change of the outflow port. This suggests that the airflow change near the outflow port may be caused by this swirl.

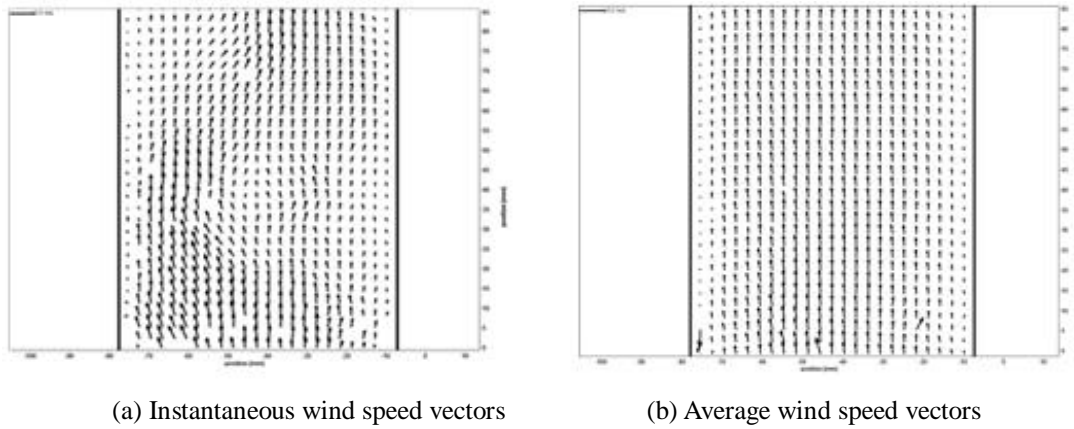


Figure9. Wind speed vectors in central part of SVU (DC fan voltage: 6 V)

Airflow Change at the Central Part of an SVU

Figure 9 shows the instantaneous wind speed vectors and average wind speed vector distribution diagram at the central part of the SVU at 6 V. A loose undulation can be seen in the flow of the instantaneous wind speed vector in Figure 9 (a), but there is no occurrence of an unexpected swirl. In addition, no swirl or major flow change was seen in any of the images captured. As Figure 9 (b) shows, the average wind speed vectors indicate that the velocity at the central part is high, and on the wall side there is a symmetrical uniform flow with decreasing velocity. The velocity difference between the centre of the flow and the wall side changes, but a similar result was seen at 12 V and 24 V as well. Therefore, the central part of

the SVU has a relatively stable airflow distribution in the velocity field of this experiment. When designing soundproofing for the central part of the SVU, it is essential to not disturb the central flow.

Comparison between PIV and Hot Wire Anemometer

We analysed the measurement accuracy by comparing the measurement values of PIV and the hot wire anemometer. Figure 10 shows the measurement results for PIV and the hot wire anemometer at the outflow port. The measurement result with PIV has a very high number of measurement points, and there are even some examples that are oscillating. Hence, to confirm a qualitative trend, we plotted only one-quarter of the total measurement points in the diagram.

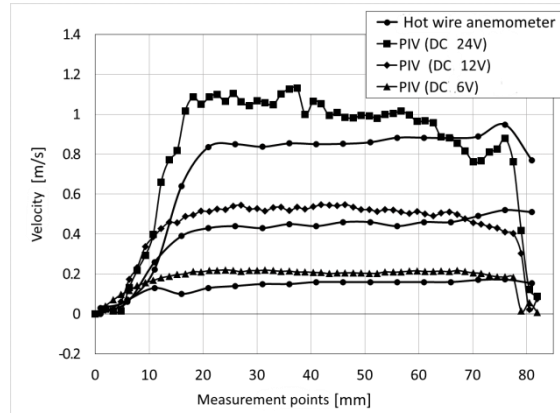


Figure10. Comparison of measurement values with PIV and hot wire anemometer at outflow port

As Figure 10 shows, the PIV results in all velocity areas have higher numbers than those with the hot wire anemometer. The difference is particularly large at the lower end of the outflow port (0 to 20 mm), where the velocity gradient is large. It is also possible to notice that the difference tends to increase as the inflow velocity increases. Two possible reasons include the difference in measurement time and

underestimation of the hot wire anemometer. In this experiment, while the wind speed with PIV is an average of 2 s, with the hot wire anemometer, we averaged 30 pieces of data (30 s) for a single point. Therefore, the measurement value with the hot wire anemometer is better averaged than that with PIV. Consequently, the value of the hot wire anemometer may have become smaller and generated the difference. It

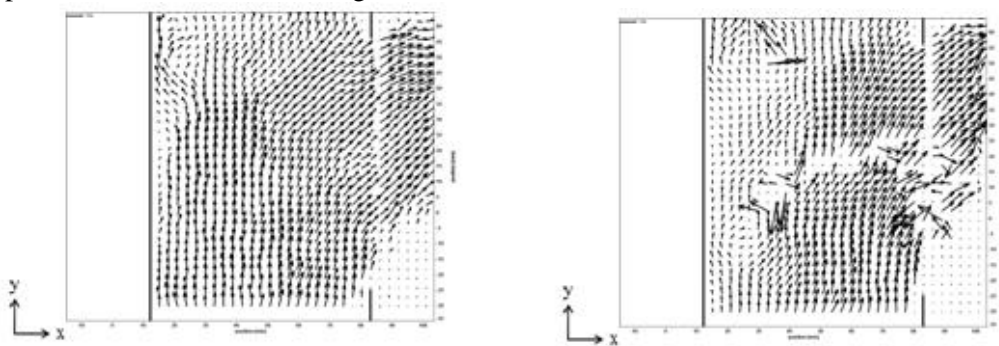
is also possible that the structure of the hot wire anemometer could not capture the entire wind speed in the Y direction and underestimated the synthesis rate.

Measurement Value Changes according to Measurement Conditions

In order to analyse the influence of the laser pulse interval on the generation of vectors and measurement results, we generated a distribution diagram of instantaneous wind speed vectors at 24 V with the conditions indicated in Table 1, changing only the laser pulse interval. The result is shown in Figure 11, and the measurement values at the outflow port are shown in Figure 12.

Figure 11 is a comparison between two examples of images of the instantaneous wind speed vector distribution diagram at different

laser pulse intervals obtained at the same time. As Figure 11(a) shows, at 200 μ s, the result is well arranged, with no erroneous or missing vectors. In Figure 11(b), at 500 μ s, there are missing and erroneous vectors, and although we omit the diagram, a similar result was obtained at 800 μ s. In addition, from Figure 12, we can see that these influences directly produce a large error in the measurement value. This is because at a velocity of 24 V and with intervals higher than 500 μ s, the moving distance of the particles becomes longer than the analysis area. As a consequence, it is not possible to calculate the movement amount of the particles with accuracy in the analysis. Therefore, with these experimental conditions and a wind speed of 24 V or higher, it is necessary to set the laser pulse interval at shorter than 200 μ s.



(a) Instantaneous wind speed vector distribution at 200 μ s (b) Instantaneous wind speed vector distribution at 500 μ s

Figure 11. Change in vectors at different laser pulse intervals (DC fan voltage: 24 V)

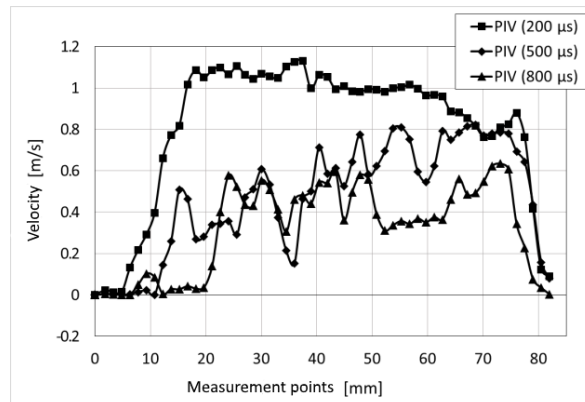


Figure 12. Changes in measurement values at different laser pulse intervals (DC fan voltage: 24 V)

We omit the diagram, but with a voltage of 6 V and 12 V, a well-arranged airflow distribution was observed with no erroneous instantaneous wind speed vectors at any laser pulse interval. Further, we compared the measurement value with different laser pulse intervals; however, no significant difference was observed.

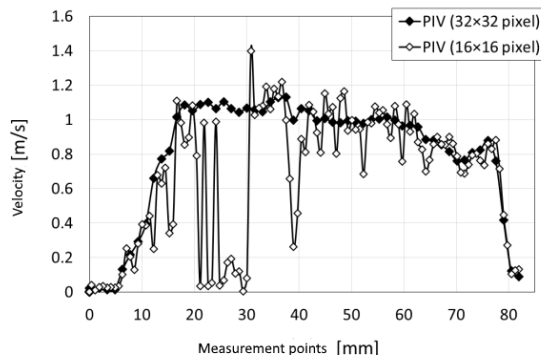
Therefore, if the movement of the particle is captured within the analysis area, even if the

laser pulse interval is changed, the measurement value is not affected.

Influence of the Analysis Area

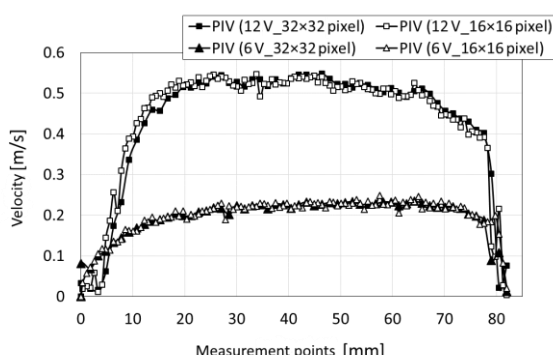
A correlation coefficient is obtained in the analysis area. The spatial resolution can be improved by reducing the size of this area. To determine the influence of the dimensions of the analysis area on the measurement result, we carried out a measurement with the previously

mentioned conditions and a different analysis. The results are depicted in Figure 13. These diagrams were generated from images obtained



(a) Measurement results of outflow port at 24 V

from the same shooting; only the analysis area was different.



(b) Measurement result of outflow port at 6 V and 12 V

Figure13. Comparison of measurement results with different analysis areas

Figure 13 (a) shows that at 24 V, when the analysis area is changed from 32×32 to 16×16 pixels, it causes a large fluctuation in the measurement value. When the analysis area was reduced, it was no longer possible to capture particle movements that were captured with 32×32 pixels. As a result, it was no longer possible to measure it with accuracy. Therefore, to run an analysis with 16×16 pixels, it is necessary to set the laser pulse interval to less than 200 μ s so that the movement amount of the particles can be captured in detail.

From Figure 13 (b), it can be noted that at 6 V and 12 V, even if the analysis area is changed, the measurement values are not affected. Based on these results, we were able to confirm that, in this experiment, when the movement amount of the particles is being captured with accuracy, reducing the analysis area from 32×32 to 16×16 pixels does not lead to higher measurement accuracy. Therefore, for the velocity area of this experiment, an analysis area of 32×32 pixels is more appropriate.

CONCLUSION

By measuring the airflow at three different spots of an SVU with PIV, we verified the airflow distribution inside the SVU at each inflow velocity. In addition, by comparing the measurement result at the outflow port with PIV and a hot wire anemometer, we verified the measurement accuracy. Finally, we changed the laser pulse interval and analysis area to verify how they affect the measurement values. From these procedures, we obtained the following conclusions:

- In the region near the outflow port of the SVU, a periodic flow change occurs, and the period changes according to the inflow velocity.
- A swirl is formed at the top of the SVU. The position at which the swirl occurs changes according to the inflow velocity. In addition, the swirl is likely to be caused by the airflow change near the outflow port.
- In the central part of the SVU, a relatively stable airflow distribution is observed regardless of the inflow velocity.
- In the measurement results with PIV and a hot wire anemometer, PIV showed overall higher values than the hot wire anemometer. A possible reason is that owing to the difference in measurement time, the measurement value with the hot wire anemometer was more averaged than that with PIV, resulting in a lower number. Moreover, it is possible that the synthesis rate was underestimated owing to the structure of the hot wire anemometer.
- We changed the laser pulse interval and analysis area to verify their effect on the measurement values; however, under these experimental conditions, we observed no improvement in measurement accuracy.
- In the future, we hope that the airflow distribution inside an SVU obtained through this experiment leads to research on the shape and installation position of noise-absorbing materials and partition boards that have little influence on the flow, as well as observations of the airflow distribution when these are installed.

REFERENCES

- [1] H. Y. T. Phan, T. Yano, H. A. T. Phan, T. Nishimura, T. Sato, Y. Hashimoto, Community responses to road traffic noise in Hanoi and Ho Chi Minh City, *Applied Acoustics*, Vol. 71(2), (2010), pp. 107–114.
- [2] H. A. T. Phan, T. Yano, H. Y. T. Phan, T. Nishimura, T. Sato, Y. Hashimoto, Annoyance caused by road traffic noise with and without horn sounds, *Acoustical Science and Technology*, Vol. 30(5), (2009), pp. 327–337.
- [3] T. Nasu and T. Nishimura, Acoustic Characteristics of a Soundproofing Unit Having an Inlet and Outlet Located on the Crossed Right Angle Face, *Journal of Environmental Engineering (Transactions of AIJ)*, Vol. 80(716), (2015), pp. 887–896.
- [4] Visualization Society of Japan, *Handbook of particle image velocimetry*, Morikita Publishing Co., Ltd., (2002).
- [5] Shin-ichi Akabayashi, Jun Sakaguchi, Takayuki Kakuma, and Xiaoyun Yang, Basic Study on the Measuring Method of the Indoor Air flow by PIV (Part 1: Study on the most suitable Seeding Conditions, *Architectural Institute of Japan/Hokuriku Branch Research Report Collection*, Vol. 54, (2011), pp. 207–210.
- [6] Hiroshi Nakajima, Yasushi Kondo, Koji Ibaraki, PIV Measurement of Supplied Airflow from Air Diffuser and Accuracy Validation, *Technical Papers of Annual Meeting, the Society of Heating, Air-Conditioning and Sanitary Engineers of Japan*, (2011), pp. 173–176.

Citation: *T. Yuichi, H. Norihiro, M. Keisuke, N. Sohei and T. Teiichi, "Construction of Experimental Method for Airflow Analysis inside a Soundproofing Ventilation Unit", International Journal of Emerging Engineering Research and Technology, vol. 6, no. 1, pp. 56-63, 2018.*

Copyright: © 2018 T. Yuichi, et al. This is an open-access article distributed under the terms of the Creative Commons Attribution License, which permits unrestricted use, distribution, and reproduction in any medium, provided the original author and source are credited.